ENVIRONMENTAL RESEARCH
LETTERS

LETTER • OPEN ACCESS

Recent increasing frequency of compound summer drought and heatwaves in Southeast Brazil

ENVIRONMENTAL RESEARCH
LETTERS

OPEN ACCESS

RECEIVED
10 November 2020

REVISED
15 January 2021

ACCEPTED FOR PUBLICATION
28 January 2021

PUBLISHED
25 February 2021

LETTER

Recent increasing frequency of compound summer drought and heatwaves in Southeast Brazil

João L Geirinhas[1], Ana Russo[1], Renata Libonati[2,1], Pedro M Sousa[1], Diego G Miralles[3] and Ricardo M Trigo[1,2]

[1] Instituto Dom Luiz (IDL), Faculdade de Ciências, Universidade de Lisboa, 1749-016 Lisboa, Portugal
[2] Departamento de Meteorologia, Universidade Federal do Rio de Janeiro, Rio de Janeiro 21941-919, Brazil
[3] Hydro-Climate Extremes Lab (H-CEL), Ghent University, Ghent, Belgium

E-mail: jlgeirinhas@fc.ul.pt

Keywords: Southeast Brazil, compound events, droughts, heatwaves, climate extremes

Supplementary material for this article is available online

Abstract

An increase in the frequency of extremely hot and dry events has been experienced over the past few decades in South America, and particularly in Brazil. Regional climate change projections indicate a future aggravation of this trend. However, a comprehensive characterization of drought and heatwave compound events, as well as of the main land–atmosphere mechanisms involved, is still lacking for most of South America. This study aims to fill this gap, assessing for the first time the historical evolution of compound summer drought and heatwave events for the heavily populated region of Southeast Brazil and for the period of 1980–2018. The main goal is to undertake a detailed analysis of the surface and synoptic conditions, as well as of the land–atmosphere coupling processes that led to the occurrence of individual and compound dry and hot extremes. Our results confirm that the São Paulo, Rio de Janeiro and Minas Gerais states have recorded pronounced and statistically significant increases in the number of compound summer drought and heatwave episodes. In particular, the last decade was characterized by two austral summer seasons (2013/14 and 2014/15) with outstanding concurrent drought and heatwave conditions stemmed by severe precipitation deficits and a higher-than-average occurrence of blocking patterns. As result of these land and atmosphere conditions, a high coupling (water-limited) regime was imposed, promoting the re-amplification of hot spells that resulted in mega heatwave episodes. Our findings reveal a substantial contribution of persistent dry conditions to heatwave episodes, highlighting the vulnerability of the region to climate change.

1. Introduction

Positive trends in the frequency and severity of compound drought and heatwave (CDH) events have been reported for numerous regions of the world, including USA [1, 2], Europe [3, 4], Australia [5] and China [6, 7]. The progressive intensification of these compound extremes represents one of the largest challenges in climate change [8, 9], and may be responsible for a wide range of natural and socio-economic impacts, such as heat-related mortality [10], severe wildfires [11], air pollution [12], agricultural losses [13], and water and energy shortages [14, 15].

It is now accepted that the univariate analysis of a single climate event typically underestimates the effect of the combination of climatic extremes over different spatial and temporal scales [1, 16]. In the case of hot and dry extreme episodes, the influence of local [17] and remote [18] land–atmosphere feedbacks contributes to their simultaneous occurrence. These feedbacks control the local temperature escalation via surface sensible heat from the drying soils; moreover, temperature anomalies can be propagated downwind via heat advection [18, 19]. The inter-links between droughts and heatwaves are however, still under study, both in terms of atmospheric drivers and land–atmosphere coupling [19]. Recent studies

have characterized hot and dry compound extremes based on distinct approaches, including event coincidence analysis [20, 21], frequency of simultaneous occurrences of multiple extremes [22], or copula analyses [23].

South America (SA), and particularly Southeast Brazil (SEB), has experienced over the past few decades an increase in the frequency, intensity and duration of extremely hot and dry events [24, 25]. Recently, Perkins-Kirkpatrick and Lewis [26] showed that significant positive trends regarding the intensity and duration of the longest heatwaves per year were recorded for SA, and particularly SEB, over the period 1950–2014. Silva Dias *et al* [27], showed a temperature increase of more than 3 °C between 1940 and 2010 for the SEB mega-city of São Paulo (SP), that after the 80s decade also registered a significant increase in the number of heatwaves [28]. Positive trends in vapor pressure deficit have been also observed during the past decades in the Southeast Amazon region and SEB, pointing for a higher influence of land–atmosphere coupling under warmer climate [29]. Cunha *et al* [30] demonstrated that most Brazilian regions experienced in the last decade the most severe droughts over the past 60 years. This concentration of events involved unprecedented drought conditions in SEB during the austral summer seasons of 2013/14 and 2014/15 [31, 32]. These prolonged periods with lack of precipitation were responsible for catastrophic impacts in water availability for human consumption and hydropower generation [30]. Between January 2014 and February 2015, an unprecedented number of forest fires were recorded in the mountainous region of Rio de Janeiro (RJ) [33]. Additionally, a dramatic excess of fatalities was recorded in the region due to a severe dengue fever outbreak, linked to home water storage tanks installed by the population [34, 35]. The severe water scarcity in SEB also led to significant impacts on economy, with the coffee production sector suffering great losses [36, 37].

Climate projections indicate a continuing intensification of these extreme events in a separate mode and, particularly, in a compound manner [24, 25]. Despite the scientific progress to date, the full comprehension of the mechanistic links between heatwaves and drought is in its early stages [19]. Conceptual and technical barriers remain, such as the ambiguity in drought and heatwave definitions [38], limitations of data products [5], and challenges in the characterization of causal links across the land–atmosphere interplay [19]. This is paramount for the SEB region considering that, despite a few recent exceptions [39], the region still lacks a comprehensive assessment of CDH events and their impacts. In addition, SEB is a heavily populated area responsible for 60% of the total Brazilian gross domestic product. In 2018, the population in SEB—which encompasses the Mega Metropolitan Regions of SP, RJ, and Belo Horizonte, capitals of SP, RJ and Minas Gerais (MG) states, respectively—reached 87 million, representing 42% of the total Brazilian population [40].

This study aims to (a) analyse the historical evolution of CDH events in SEB, (b) characterize the land and atmosphere conditions, and (c) disentangle the physical land–atmosphere coupling mechanisms, enabled by the atmospheric and surface conditions analysed in (b), that were responsible for the observed record-breaking dry and hot events recorded during the 2013/2014 and 2014/2015 summers.

2. Data and methods

2.1. Data

Daily and hourly meteorological data, including maximum temperature (T_{max}), precipitation, 500 hPa geopotential height (Z500), surface net solar radiation and surface sensible heat flux values were extracted from the European Centre of Medium-range Weather Forecast ERA-5 reanalysis datasets (Copernicus Climate Change Service—C2S, 2017) [41]. Soil moisture data were obtained from the Global Land Evaporation Amsterdam Model (GLEAM v3.3a) [42, 43]. All variables were retrieved for the summer season (December–February) using the 1980–2018 base period, at a gridded 0.25° × 0.25° spatial resolution, and for a selected area encompassing SEB (14–26° S, 54–38° W) (figure 1).

2.2. Compound drought and heatwave definition and indices

Drought conditions were defined at a monthly scale and considering 3 month Standardized Precipitation Index (SPI) values <-1 [44]. Heatwave events were identified using a relative threshold methodology [38], considering periods of consecutive days with T_{max} values above a certain percentile of T_{max} for the particular calendar day (calculated on a 15 day window). Different percentiles (80th, 90th, 95th) and durations (3–4 days, 5–7 days, >7 days) were considered. In order to isolate T_{max} values from the global warming effect, the linear trend was removed from the entire time series by applying a 1st degree polynomial regression technique.

Considering the above-mentioned criteria for the definition of monthly drought and daily heatwave periods, a CDH event was defined as a heatwave episode that occurs during a month under drought conditions (i.e. a month with an associated 3 month SPI value <-1). This is a simple and effective compound event metric that was already used in previous studies [1] and that safeguards the inherent and different time-scales linked to the definition of both extremes. To quantify the historical change of CDH events for each SEB grid-cell, we derived a percent (%) change index. This percent change is defined as the difference between the number of compound events recorded during the 1999/00–2017/18 and 1980/81–1998/99 summer seasons, normalized

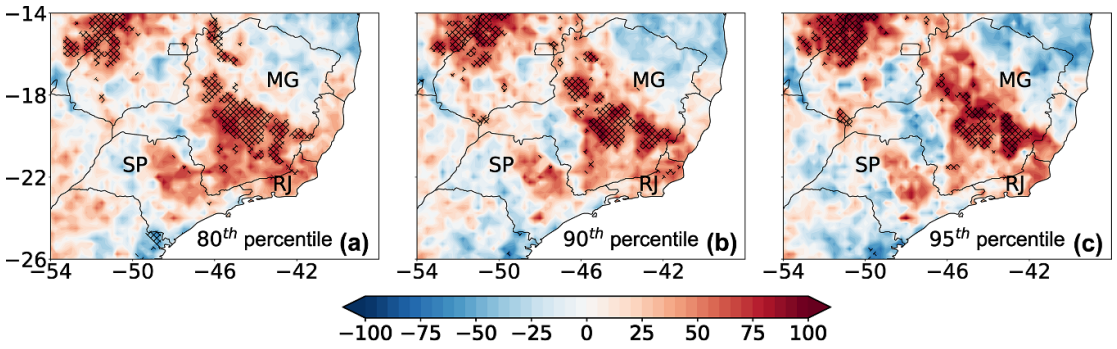

Figure 1. Percent change (%) in CDH events (all events considered, with durations of at least three consecutive days) during 1999/00–2017/18 summer seasons (DJF) relative to 1980/81–1998/99 summer seasons. Each panel shows a different heatwave severity, based on (a) 80th, (b) 90th and (c) 95th temperature percentile thresholds. Statistically significant ($p < 0.05$) percentage changes are identified by thin black crosses.

by the total number of events identified throughout the whole analysis period. In order to assess the statistical robustness of the above mentioned percent change values, a non-parametric Wilcoxon Rank Sum test [45] was computed. This statistical test assesses the significance between pairs of data that are non-normally distributed. In this particular analysis, the annual CDH events observed during the 1980/81–1998/99 and 1999/00–2017/18 summer seasons were defined as the pairs of data to be tested. Finally, the percent change values were considered as statistically significant if they were result of two pairs of data with different median values. The percentage of total summer pixels under a compound regime was also analysed. This methodology follows the approach applied to the USA by Mazdiyasni and AghaKouchak [1], and it is obtained by calculating the percentage of total number of pixels for each summer season that are in CDH conditions:

$$\text{pixels}_{\text{total}} = \text{pixels}_{\text{lat}} \times \text{pixels}_{\text{lon}} \times \text{pixels}_{\text{time}} \quad (1)$$

lat and lon represent, respectively, the number of pixels in latitude and longitude, and time represents the number of days within each summer season. For instance, a percentage of 100% indicates that concurrence conditions were recorded for the entire SEB area as well as during all summer days.

2.3. Definition of atmospheric blocking anomalies

Regional atmospheric blocking was detected by searching reversals of the usual Z500 gradient. Instantaneous (at the daily scale) local blocking was defined by detecting grid-cells presenting simultaneously negative Z500 gradient towards 15° north and 15° south, i.e. meridional maxima of Z500 [46]. These daily detections were used to compute monthly and seasonal climatological frequencies of regional blocking occurrence, and, subsequently, to derive monthly and seasonal relative anomalies with respect to the 1980–2018 base period.

3. Results

3.1. Historical evolution of compound episodes

We started by analysing the percent change of CDH events, considering all the summer heatwave episodes with durations above three consecutive days and three different thresholds (80th, 90th, 95th percentiles) (figure 1). During the 1999/00–2017/18 period, concurrences increased substantially (values between 50% and 100%) over the northwestern SEB section, the central and southern areas of MG, and the northeastern section of RJ. This increase is statistically significant over large swaths when compared to the 1980/81–1998/99 period. Positive values were also observed in some areas of SP, however a general absence of statistically significance was evident. All the remaining areas presented near-zero or even negative values, mostly not statistically significant. The spatial variability pattern of the percent change was very similar throughout the considered temperature thresholds.

In addition to considering different thresholds we also assessed the percent change for different heatwave durations (figure 2). Despite some slight differences regarding the spatial pattern of percent change values distribution throughout all the combinations of drought and heatwave, in general, severe and long compound events have become more frequent than those short and mild. This is particularly evident for the SEB northwestern section and MG central and southern areas. For compound event durations of 3–4 days (figures 2(a)–(c)), large parts of SEB presented positive and statistically significant ($p < 0.05$) percent changes, with the highest values in the MG central region. Regarding compound events with a duration of 5–7 days (figures 2(d)–(f)), the pattern was very similar, despite the higher absolute values of percent change. As we consider even longer heatwaves and higher intensity thresholds, the SEB area with negative percent change values also increases, although the values are typically non-statistically significant. Taking into account the longest compound

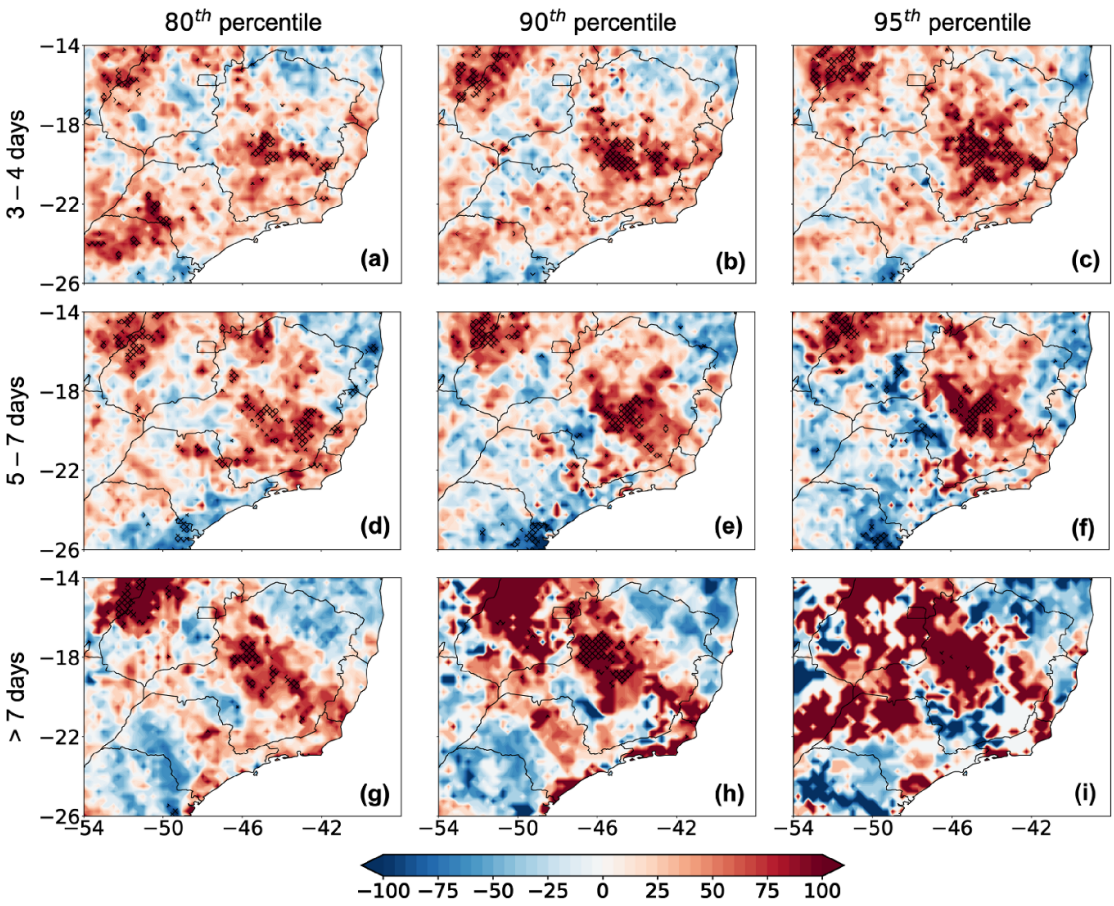

Figure 2. Percent change (%) in the occurrence of summer (DJF) CDH events during 1999/00–2017/18 relative to 1980/81–1998/99. The rows correspond to different heatwave durations (3–4, 5–6, >7 days). The columns show different heatwave severities (80th, 90th and 95th percentiles). Statistical significant ($p < 0.05$) percentage changes are identified by black crosses.

heatwave events (figures 2(g)–(i)), the regions with higher positive and statistically significant values were located within MG, which is in fact, the only SEB area that presented a robust and consistent pattern of positive % change throughout all the combinations of severity and duration of compound heatwaves. Regions such as the coastal section of RJ and some interior land parts of SP also presented positive changes close to 100%. However, the interpretation of these results requires a careful consideration due to their lack of statistical significance.

We looked in detail to the critical summer seasons that contributed more to the positive changes in SEB. In each one of the three most populated states (namely SP, MG and RJ), the percentage values of total summer pixels under a compound regime were also analysed (see section 2 and figure 3). To consider as many compound events as possible, the percentage levels were computed using the lowest heatwave percentile threshold (80th) and a duration of at least 3 days. Considering the whole SEB area, the most critical summer seasons in terms of concurrence percentage were observed during the last decade of the period under analysis, particularly during the summers seasons of 2013/14, 2014/15 and 2015/16, when the combined values were about 20% (figure 3, black curve). The severe conditions observed during the 2013/14 summer season were largely explained by the percentage of concurrence recorded for SP (>40%). The high percentage of concurrence observed for RJ (near 50%) and for MG (30%) is likely to explain the values observed during the 2014/15 summer season over the whole SEB. Throughout the first half of the analysis period (1980–1999), relatively high SEB concurrence was also recorded, particularly during the 1983/84 and 1985/86 seasons. For the latter, SP recorded the second-highest percentage of concurrence in the analysis period (near 30%). Similarly, RJ showed a relatively high percentage of concurrence during the first half of the period, in particular during the 1983/84, 1989/90 and 1995/96 seasons. For the state of MG was also evident the high percentage of concurrence during the last decade of the analysis period, supporting the results shown in figure 1, where MG was the only SEB area with a consistently and statistically significant increase in CDH events. In short, it is unquestionable that the three summer seasons between 2013 and 2016 were characterized by the most severe CDH events although with some different spatial incidence from season to season.

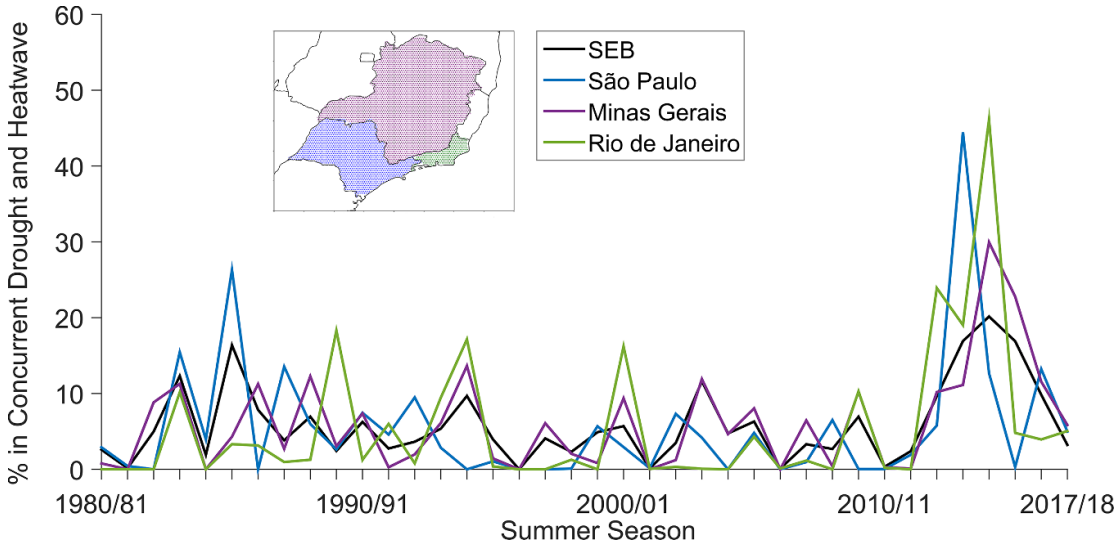

Figure 3. Percentage of total yearly summer pixels (%) under a CDH regime (heatwave defined using a 80th percentile threshold and a duration of at least three consecutive days) from 1980/81 to 2017/18 and for different spatial domains: whole SEB, the states of São Paulo, Rio de Janeiro, and Minas Gerais (black, blue, green and purple lines, respectively).

3.2. The record-breaking 2013/14 and 2014/15 summer seasons

3.2.1. Land and atmosphere characterization

The unprecedented CDH situation observed during 2013/14, particularly for SP, and during 2014/15 particularly for RJ and MG, deserves the analysis of the atmospheric synoptic conditions, the land surface drivers and the soil–atmosphere coupling mechanisms. Figure 4(a) represents the yearly summer precipitation anomalies from 1980/81 to 2017/18. During the last quarter of the analysis period, the three states presented a marked correspondence between drought–heatwave concurrence and precipitation deficits (figures 3 and 4(a)). For SP, the negative association was more evident for the 2013/14 summer season, when the lowest ever recorded negative precipitation anomaly (figure 4(a)) corresponded to the highest concurrence percentage (figure 3). Regarding the states of MG and RJ, this particular summer season was also characterized by an extreme absence of precipitation. In fact, the precipitation anomaly in RJ was very similar to that in SP, however, the SP percentage of concurrence was far greater (figure 3). Figure 4(b) shows a different perspective on surface dryness for the different states. Severe and historically unprecedented drought conditions were observed over SP in 2013/14, while in MG and RJ soil moisture anomalies were closer to zero, or even positive in some areas. This indicates that, although these regions experienced similar conditions in terms of mean summer precipitation deficits (figure 4(a)), the surface was considerably drier in SP. This asymmetry between the three states was likely due the occurrence of different precipitation episodes in these three states and to greater evaporation rates in SP, promoted by higher shortwave radiance incidence at surface. The later was linked to anticyclonic conditions promoting clear skies and high diabatic heating (figures 4(d) and S1 (available online at stacks.iop.org/ERL/16/034036/mmedia)). In fact, looking at the large-scale atmospheric circulation, we found that during the 2013/14 summer season SP experienced a higher than normal percentage of days under atmospheric blocking than MG and RJ (figure 4(d)). These quasi-stationary anticyclonic circulation patterns are prone to higher than average incidence levels of solar radiation at surface [47, 48], and ideal to foster evaporation—as long as soil moisture is still available—progressively drying the soils and favouring the escalation of temperatures through diabatic heating [48]. Figure S1 corroborates this point, showing the incidence of high levels of solar incoming radiation, particularly over SP. Therefore, the different synoptic atmospheric conditions experienced by SP, MG and RJ were essential to explain the differences among soil moisture levels (figure 4(b)), the number of heatwaves, and the percentages of concurrence (figure 3).

For MG and RJ, the lowest (highest) recorded precipitation anomaly (percentage of concurrence) was observed during the 2014/15 summer season. Despite this, the precipitation anomaly values were not so different compared to 2013/14. By contrast, soil moisture anomalies (figure 4(c)) were much stronger and widespread in MG and RJ when compared to the 2013/14 season (figure 4(b)). This difference reflects the fact that during the period between the 2013/14 and 2014/15 summer seasons, pronounced precipitation deficits were maintained, particularly for MG and RJ [49]. Consequently, the soil moisture values continued to decrease at a faster rate in these two states, compared to SP. Secondly, the synoptic

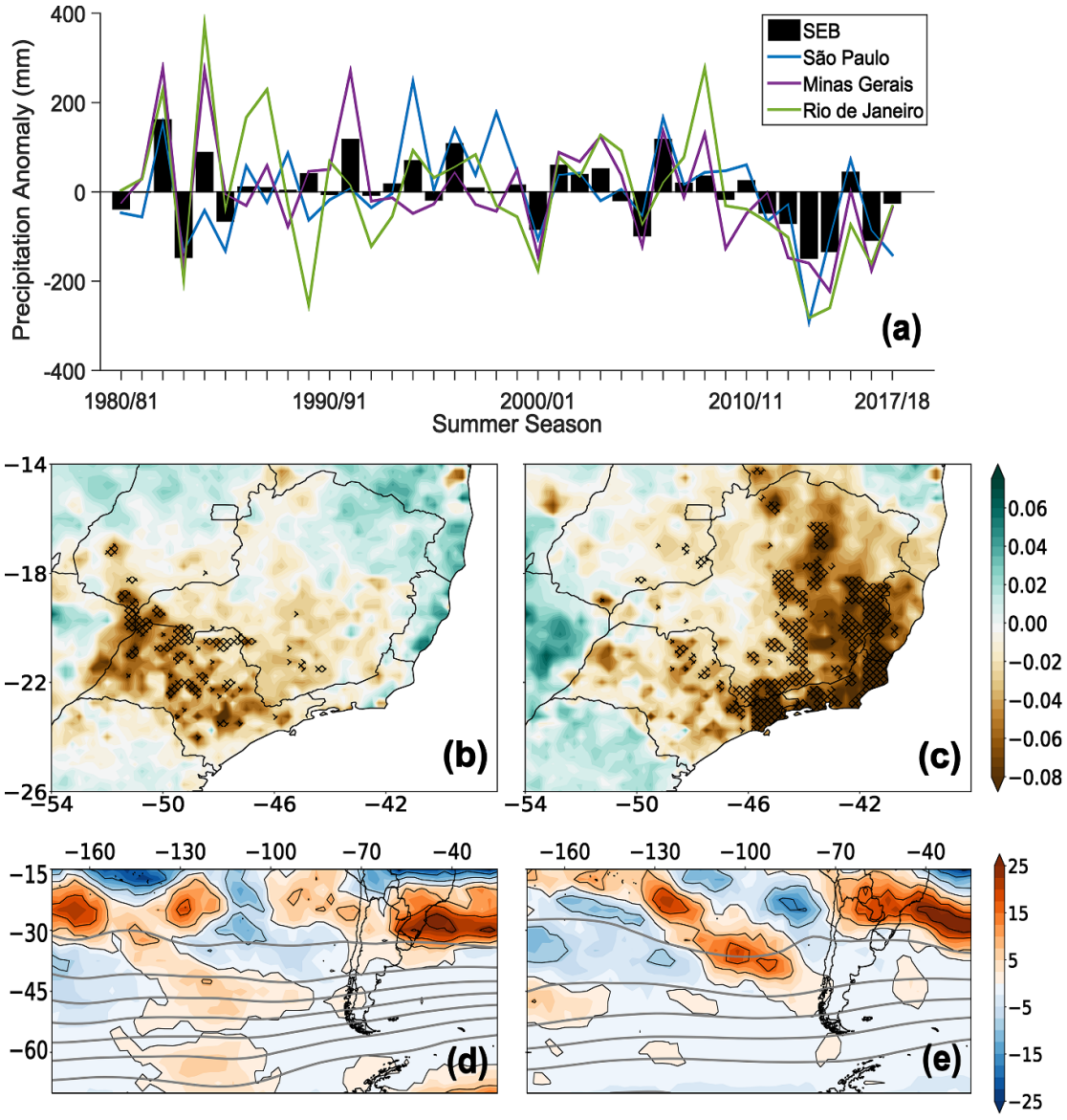

Figure 4. (a) Area average austral summer precipitation anomaly time series for SEB, SP, RJ and MG. (b) and (c) Soil moisture anomaly values regarding summer climatology ($m^3_{H_2O}/m^3_{soil}$) during the 2013/14 (b) and the 2014/15 (c) summer seasons. Regions marked with crosses denote the areas in which the negative anomalies where the lowest ever recorded within the analysis period (1980–2018). (d) and (e) Relative anomaly in the percentage of summer days (colors, %) affected by atmospheric blocking conditions and summer averaged 500 hpa geopotential height field (gray contour lines delimitating equal geopotential areas) during the 2013/14 (d) and the 2014/15 (e) summer seasons, respectively.

atmospheric circulation pattern in MG and RJ, contrary to SP, induced clear sky conditions and strong diabatic heating, leveraging initially high evaporation rates (until soil dry-out) and the occurrence of several heatwave periods, and, consequently, compound events. During the 2014/15 season the predominant atmospheric blocking pattern (figure 4(e)) moved northeast, affecting a broader area in RJ and MG when compared to the 2013/14 season (figure 4(d)). Consequently, clear sky conditions were predominant over these two states, offering the ideal conditions (radiative forcing and diabatic heating) for boosting the development of heatwaves over RJ and MG, rather than over SP (figure S1). Analysing the isohypses at 500 hpa during the 2014/15 summer season (figure 4(e)), it is possible to observe a well-defined wave pattern of the mid-atmosphere circulation spanning from the central south Pacific Ocean to the western South Atlantic Ocean and to the vicinities of south and southeastern coast of Brazil. This ridge-trough sequence was a clear signature of a large-scale teleconnection wave train that was also identified (although with less intensity) during 2013/14 (figure 4(d)). This Rossby wave train was induced by an equatorial Pacific heat source north of Australia [31].

3.2.2. The land–atmosphere coupling mechanisms

To characterize the land–atmosphere interactions responsible for the potential reinforcement of hot and

dry events [1, 17, 19], the anomaly time series of near-surface air temperature, surface net solar radiation, soil moisture and sensible heat flux were analysed in detail for the three SEB states. Figure 5 shows the results of this analysis for the 2013/14 summer season, highlighting several periods defined by positive anomalies of 2m air temperature, particularly in SP. The first period appeared during the first days of December 2013 (3rd–5th) and was primarily promoted by a strong diabatic process represented by positive anomalies of surface net solar radiation. The summer season started with positive soil moisture anomalies and, consequently, negative anomalies of sensible heat fluxes were not recorded. It is important to note that ECMWF convention for vertical radiative fluxes is negative upwards and positive downwards. The summer season progressed under a pronounced lack of precipitation, especially over SP, promoting a steady decrease in soil moisture. From the last days of December until mid-January another hot period was recorded, presenting a close association with positive anomalies of surface net solar radiation. The meteorological situation of clear sky conditions and precipitation deficits remained until the mega-heatwave event over SP, from January 20th to February 15th. The pronounced variation of the accumulated values from all the analysed parameters reflects the magnitude of this episode (see bold lines in figure 5). Initially, the positive temperature anomalies were induced by strong diabatic contributions that promoted a sharp decrease in soil moisture due to a high evaporative demand. As the availability of water on the surface reduced, the surface started to deliver part of the available radiative energy back to the atmosphere through sensible heat fluxes, further intensifying the temperatures. During 2014/15, the role played by land–atmosphere coupling was larger in RJ and MG compared to SP (figure S2).

In contrast to the 2013/14 summer season, the soil moisture anomalies during the beginning of the 2014/15 season were already negative, reflecting antecedent precipitation anomalies, and continued to decrease as the season progressed. This led to pronounced anomalies in surface sensible heat fluxes. This land–atmosphere coupling was evident for RJ during the whole month of December and January, especially when diabatic forcing conditions were met. Regarding MG, the coupling process was more intense throughout the entire month of January 2015.

4. Discussion and conclusion

Until this study, the physical mechanisms responsible for triggering the amplification of CDH events remained unclear for SEB, particularly with respect to (a) the level to which heatwaves, as recurrent isolated events causing heat-stress, could enhance already established drought conditions, (b) the extent to which prolonged drought and subsequent surface sensible heat fluxes can amplify heatwaves, and (c) the degree to which (a) and (b) can concur. The summer seasons of 2013/14 and 2014/15 were clear examples of such an association between drought and heatwave in this important region of Brazil. This inter-relationship was controlled by two soil–atmosphere coupling regimes that were predominant during distinct periods of both summer seasons, and defined by pronounced evaporative demands and different evaporation levels and soil moisture availability [50]. The first regime (energy-limited), characterized by a low coupling, occurred during the first half of both summer seasons, in which consecutive hot periods coupled with long-term precipitation deficits were important to induce the dry surface conditions. During the hot periods, the demand of the atmosphere induced by the clear sky conditions and low humidity levels was satisfied by increasing evaporation rates and, consequently, the soil moisture availability suffered an accelerated decrease (figures 5(c) and S2). The ideal synoptic conditions for high levels of shortwave radiation incidence were maintained and, due to a severe dryness of the surface, a high coupling regime (water-limited) was imposed, in which the heatwave events were amplified by the simultaneous drought conditions. In this second regime, the evaporative demand continued to increase. However, contrary to the first regime, evaporation rapidly decreased. This was due to an absence of soil water availability, and so, the surface started to lose its capability to meet the atmospheric water demand. Relying in previous conducted analysis, it is likely that the transpiration declined as plant stomata closed to prevent desiccation [19, 51], not just as a response to the low soil water content, but also to the high atmospheric vapour pressure deficit. At this stage, the surface started to disproportionally dissipate the incoming radiation as sensible heat, instead of latent heat (evaporation). Consequently, near surface atmospheric temperatures further escalated, increasing the severity of the events, and leading to mega-heatwaves such as the ones we recorded for SEB. Therefore, the presence of the observed higher-than-average blocking patterns over SEB during the 2013/14 and 2014/15 summer seasons—responsible for reduced cloudiness, large precipitation deficits, advection of warm air and a high atmospheric demand for humidity—proved to be essential for soil moisture depletion, yielding large fluxes of sensible heat and a subsequent reduction in evaporative cooling. These persistent synoptic conditions likely resulted, therefore, in the progressive intensification of drought and heatwave conditions.

For Europe, it has been demonstrated that conditions of dry soils can also intensify heat entrainment from the top of the atmospheric boundary layer and favour the near-surface multiday storage of heat in the residual boundary layer [17]. Model experiments have also shown the potential of soil dryness to

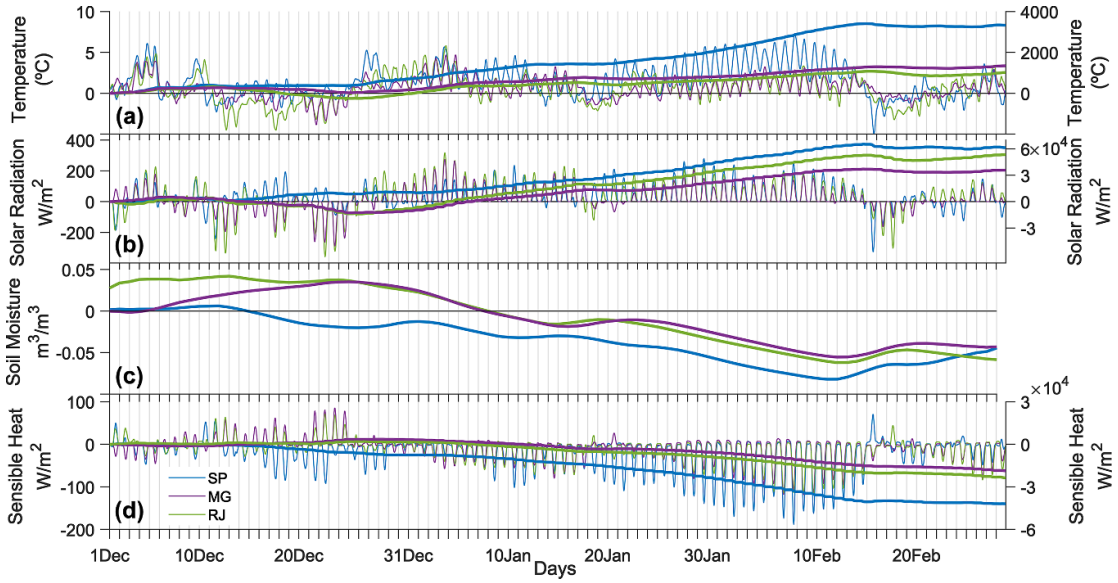

Figure 5. Anomalies (left *y*-axis) from 1st December of 2013 to 28th February of 2014, of (a) surface 2m temperature (at a hourly scale), (b) surface net solar radiation (at a hourly scale), (c) soil moisture (at a daily scale) and (d) surface sensible heat flux (at a hourly scale) for SP (blue line), MG (purple line) and RJ (green line). The respective colored bold lines represent the accumulated values of each variable since 1st December (right *y*-axis).

sustain anticyclones, and consequently intensify heatwave periods [52]. Moreover, soil desiccation upwind has also been shown to increase the temperature escalation in downwind locations via heat advection [18, 53]. Most of these previous studies have concentrated in Europe, North America and Australia [1–5]. While heatwave–drought concurrence over SEB has been much less studied, recent analyses have shown that the synoptic-scale high-pressure conditions are required to generate these compound events in SEB [28, 39]. In addition, these events are related to teleconnections perturbations of inter-tropical oceanic/atmospheric modes, such as the Madden–Julian oscillation [54] and the El Niño–Southern oscillation [37, 55].

Regarding the historical evolution of these events, it is possible to conclude from our analyses that, besides the northwestern SEB section, also central MG, RJ and some areas of SP close to MG and RJ, experienced an increase in frequency. This concurrence increase proved to be more intense as we considered the most extreme and longer-lasting heatwave classes. However a careful consideration should be raised to the lack of statistical robustness among the observed percent change values, particularly for the severest and longest CDH events. Considering that the linear positive effect of global warming in T_{max} levels was accounted by removing the trend from the time series, this result indicates an increase of daily T_{max} extreme values through an increase of the time series variability. This could be explained by a growing role by dry surface conditions in generating and enhancing temperature extremes over the last years. Therefore, one of the main conclusions is that over the last decades temperatures and extreme dry and hot conditions have intensified over the densely populated SEB. These results are in accordance with previous studies for other regions worldwide [24, 28, 30, 56].

Nowadays it is well known the existence of a wide-range of impacts associated to CDH events, not just within natural sectors and ecosystems, but also for humans and particularly in what concerns public health [10, 14, 57]. All these impacts are expected to be exacerbated in a future hotter climate scenario triggered by the emissions of Greenhouse gases and other anthropogenic factors [10, 14]. For instance, Gasparrini *et al* [10] estimated that populations living in regions like Europe, Southeast Asia and South America will record a sharp surge in heat-related impacts. This will be especially true for areas where heat-stress conditions are expected to be exacerbated due to a joint effect of a global warming trend, a higher contribution of local and or remote drought condition to temperature extremes [17, 18], and also due to a regional urban heat-island effect [58]. In regards to SEB, an increment on the occurrence of compound hot and dry events is expected, particularly in the absence of a serious decrease in the emissions of Greenhouse gases. In order to provide scientific support to policy making, studies of this type are of extreme relevance and should be further supported by national and international funding agencies.

Data availability statement

All data that support the findings of this study are included within the article (and any supplementary files).

Acknowledgments

J G acknowledges the support of COST Action (CA17109) funded by COST (European Cooperation in Science and Technology) and also FCT (Fundação para a Ciência e a Tecnologia) for the PhD Grant 2020.05198.BD. A R and R T acknowledge FCT under project IMPECAF (PTDC CTA—CLI/28902/2017) and PMS under project HOLMODRIVE (PTDC/CTA-GEO/29029/2017). RL was supported by CNPQ (Grant 05159/2018-6), by FAPERJ (Grant 202.714/2019) and acknowledges project FireCast (PCIF/GRF/0204/2017); A R, P M S and R T are also grateful by the FCT funding UIDB/50019/2020–Instituto Dom Luiz. D G M acknowledges support from the European Research Council (ERC) under Grant Agreement 715254 (DRY–2–DRY).

ORCID iDs

João L Geirinhas https://orcid.org/0000-0002-2110-4891
Ana Russo https://orcid.org/0000-0003-0042-2441
Renata Libonati https://orcid.org/0000-0001-7570-1993
Pedro M Sousa https://orcid.org/0000-0002-0296-4204
Diego G Miralles https://orcid.org/0000-0001-6186-5751
Ricardo M Trigo https://orcid.org/0000-0002-4183-9852

References

[1] Mazdiyasni O and AghaKouchack A 2015 Substantial increase in concurrent droughts and heatwaves in the United States *Proc. Natl Acad. Sci.* **112** 11484–9
[2] Alizadeh M R, Adamowski J, Nikoo M R, AghaKouchak A, Dennison P and Sadegh M 2020 A century of observations reveals increasing likelihood of continental-scale compound dry-hot extremes *Sci. Adv.* **6** eaaz4571
[3] Manning C, Widmann M, Bevacqua E, Van Loon A F, Maraun D and Vrac M 2019 Increased probability of compound long-duration dry and hot events in Europe during summer (1950–2013) *Environ. Res. Lett.* **14** 094006
[4] Russo A, Gouveia C M, Dutra E, Soares P M M and Trigo R M 2018 The synergy between drought and extremely hot summers in the Mediterranean *Environ. Res. Lett.* **14** 014011
[5] Seneviratne S I *et al* 2012 Changes in climate extremes and their impacts on the natural physical environment *Managing the Risks of Extreme Events and Disasters to Advance Climate Change Adaptation. A Special Report of Working Groups I and II of the Intergovernmental Panel on Climate Change (IPCC)* ed C B Field *et al* (Cambridge: Cambridge University Press) pp 109–230
[6] Liu Y *et al* 2015 Agriculture intensifies soil moisture decline in Northern China *Sci. Rep.* **5** 11261
[7] Lu Y, Hu H, Li C and Tian F 2018 Increasing compound events of extreme hot and dry days during growing seasons of wheat and maize in China *Sci. Rep.* **8** 16700
[8] Rasmijn L M, van der Schrier G, Bintanja R, Barkmeijer J, Sterl A and Hazeleger W 2018 Future equivalent of 2010 Russian heatwave intensified by weakening soil moisture constraints *Nat. Clim. Change* **8** 381–5
[9] Dosio A, Mentaschi L, Fischer E M and Wyser K 2018 Extreme heat waves under 1.5 °C and 2 °C global warming *Environ. Res. Lett.* **13** 0540046
[10] Gasparrini A *et al* 2017 Projections of temperature-related excess mortality under climate change scenarios *Lancet Planet. Health* **1** E360–7
[11] Brando P M *et al* 2014 Abrupt increases in Amazonian tree mortality due to drought–fire interactions *Proc. Natl Acad. Sci.* **111** 6347–52
[12] Shaposhnikov D *et al* 2014 Mortality related to air pollution with the Moscow heat wave and wildfire of 2010 *Epidemiology* **25** 359–64
[13] Zipper S C, Qiu J and Kucharik C J 2016 Drought effect on US maize and soybean production: spatiotemporal patterns and historical changes *Environ. Res. Lett.* **11** 094021
[14] Zscheischler J *et al* 2018 Future climate risk from compound events *Nat. Clim. Change* **8** 469–77
[15] Coffel E D, Keith B, Lesk C, Horton R M, Bower E, Lee J and Mankin J S 2019 Future hot and dry years worsen Nile basin water scarcity despite projected precipitation increases *Earth's Future* **7** 967–77
[16] Zscheischler J *et al* 2020 A typology of compound weather and climate events *Nat. Rev. Earth Environ.* **1** 333–47
[17] Miralles D G, Teuling A J, van Heerwaarden C C and Vilà-guerau de Arellano J 2014 Mega-heatwave temperatures due to combined soil desiccation and atmospheric heat accumulation *Nat. Geosci.* **7** 345–9
[18] Schumacher D L, Keune J, van Heerwaarden C C, Vilà-guerau de Arellano J, Teuling A J and Miralles D G 2019 Amplification of mega-heatwaves through heat torrents fueled by upwind drought *Nat. Geosci.* **12** 712–7
[19] Miralles D G, Gentine P, Seneviratne S I and Teuling A J 2019 Land–atmospheric feedbacks during droughts and heatwaves: state of the science and current challenges *Ann. N. Y. Acad. Sci.* **1436** 19–35
[20] Rammig A, Wiedermann M, Donges J F, Babst F, von Bloh W, Frank D, Thonicke K and Mahecha M D 2015 Coincidences of climate extremes and anomalous vegetation responses: comparing tree ring patterns to simulated productivity *Biogeosciences* **12** 373–85
[21] Donges J F, Schleussner C-F, Siegmund J F and Donner R V 2016 Event coincidence analysis for quantifying statistical interrelationships between event time series *Eur. Phys. J. Spec. Top.* **225** 471–87
[22] Wu X, Hao Z, Hao F, Li C and Zhang X 2019 Spatial and temporal variations of compound droughts and hot extremes in China *Atmosphere* **10** 95
[23] Ribeiro A F S *et al* 2020 Drought-related hot summers: a joint probability analysis in the Iberian Peninsula *Weather. Clim. Extremes* **30** 100279
[24] IPCC 2013 Climate change 2013: the physical science basis *Contribution of Working Group I to the Fifth Assessment Report of the Intergovernmental Panel on Climate Change* (Cambridge: Cambridge University Press)
[25] Hao Z, Hao F, Singh V P and Zhang X 2018 Changes in the severity of compound drought and hot extremes over global land areas *Environ. Res. Lett.* **13** 124022
[26] Perkins-Kirkpatrick S E and Lewis S C 2020 Increasing trends in regional heatwaves *Nat. Commun.* **11** 3357
[27] Silva Dias M A F, Dias J, Carvalho L M V, Freitas E D and Silva Dias P L 2013 Changes in extreme daily rainfall for São Paulo, Brazil *Clim. Change* **116** 705–22

[28] Geirinhas J L, Trigo R M, Libonati R, Coelho C A S and Palmeira A C 2018 Climatic and synoptic characterization of heat waves in Brazil *Int. J. Climatol.* **38** 1760–76
[29] Barkhordarian A, Saatchi S S, Behrangi A, Loikith P C and Mechoso C R 2019 A recent systematic increase in vapor pressure deficit over tropical South America *Sci. Rep.* **9** 15331
[30] Cunha A P M A *et al* 2019 Extreme droughts events over Brazil from 2011 to 2019 *Atmosphere* **10** 642
[31] Coelho C A S *et al* 2016 The 2014 southeast Brazil austral summer drought: regional scale mechanisms and teleconnections *Clim. Dyn.* **46** 3737–52
[32] Coelho C A S, Cardoso D H F and Firpo M A F 2015 Precipitation diagnostics of an exceptionally dry event in São Paulo, Brazil *Theor. Appl. Climatol.* **125** 769–84
[33] Rodrigues J A, Libonati R, Peres L F and Setzer A 2018 Burned area mapping on conservation units of mountains region of Rio de Janeiro using Landsat-8 data during the 2014 drought *Anuário Do Instituto De Geociências—UFRJ* **41** 318–27
[34] Brown L, Medlock J and Murray V 2014 Impact of drought on vector-borne diseases—how does one manage the risk? *Public Health* **128** 29–37
[35] BBC 2015 Brazil faces surge in number of dengue fever cases *BBC News* (available at: www.bbc.com/news/world-latin-america-32589268)
[36] Watson K 2014 Drought hits Brazil's coffee industry *BBC News* (available at: www.bbc.com/news/business-27623535)
[37] Rodrigues R R, Taschetto A S, Sen Gupta A and Foltz G R 2019 Common cause for severe droughts in South America and marine heatwaves in the South Atlantic *Nat. Geosci.* **12** 620–6
[38] Perkins S E and Alexander L V 2013 On the measurement of heat waves *J. Clim.* **26** 4500–17
[39] Geirinhas J L, Trigo R M, Libonati R, Castro L C O, Sousa P M, Coelho C A S, Peres L F and Magalhães M D A F M 2019 Characterizing the atmospheric conditions during the 2010 heatwave in Rio de Janeiro marked by excessive mortality rates *Sci. Total Environ.* **650** 796–808
[40] IBGE 2018 Resident population estimate by federation and municipality in 2018 (available at: http://pesquisa.in.gov.br/imprensa/jsp/visualiza/index.jsp?data=29/08/2018&jornal=515&pagina=55&totalArquivos=134)
[41] Hersbach H *et al* 2020 The ERA5 global reanalysis *Q. J. R. Meteorol. Soc.* **146** 1999–2049
[42] Marten B, Miralles D G, Lievens H, van der Schalie R, de Jeu R A M, Fernández-Prieto D, Beck H E, Dorigo W A and Verhoest N E C 2017 GLEAM v3: satellite-based land evaporation and root-zone soil moisture *Geosci. Model Dev.* **10** 1903–25
[43] Miralles D G, Holmes T R H, De Jeu R A M, Gash J H, Meesters A G C A and Dolman A J 2011 Global land-surface evaporation estimated from satellite-based observations *Hydrol. Earth Syst. Sci.* **15** 453–69
[44] World Meteorological Organization 2012 *Standardized Precipitation Index User Guide* (WMO-No. 1090) (Geneva: World Meteorological Organization)
[45] Hollander M and Wolfe D A 1999 *Nonparametric Statistical Methods* (New York: Wiley)
[46] Mendes M, Cavalcanti I F A and Herdies D L 2012 Southern Hemisphere atmospheric blocking diagnostic by ECMWF and NCEP/NCAR data *Rev. Bras. Meteorol.* **27** 263–71
[47] Meehl G A and Tebaldi C 2004 More intense, more frequent, and longer lasting heat waves in the 21st century *Science* **305** 994–7
[48] Sousa P M, Trigo R M, Barriopedro D, Soares P M M and Santos J A 2018 European temperature responses to blocking and ridge regional patterns *Clim. Dyn.* **50** 457–77
[49] Nobre C A, Marengo J A, Seluchi M E, Cuartas L A and Alves L M 2016 Some characteristics and impacts of the drought and water crisis in southeastern Brazil during 2014 and 2015 *J. Water Resour. Prot.* **8** 252–62
[50] Pendergrass A G *et al* 2020 Flash droughts present a new challenge for subseasonal-to-seasonal prediction *Nat. Clim. Change* **10** 191–9
[51] Buckley T N 2019 How do stomata respond to water status? *New Phytol.* **224** 21–36
[52] Fischer E M, Seneviratne S I, Vidale P L, Lüthi D and Schär C 2007 Soil moisture-atmosphere interactions during the 2003 European summer heat wave *J. Clim.* **20** 5081–99
[53] Vautard R, Yiou P, D'Andrea F, de Noblet N, Viovy N, Cassou C, Polcher J, Ciais P, Kageyama M and Fan Y 2007 Summertime European heat and drought waves induced by wintertime Mediterranean rainfall deficit *Geophys. Res. Lett.* **34** L07711
[54] Shimizu M H and Ambrizzi T 2016 MJO influence on ENSO effects in precipitation and temperature over South America *Theor. Appl. Climatol.* **124** 291–301
[55] Cai W *et al* 2020 Climate impacts of the El Niño-Southern oscillation on South America *Nat. Rev. Earth Environ.* **1** 215–31
[56] Abreu R C, Tett S F B, Schurer A and Rocha H R 2019 Attribution of detected temperature trends in Southeast Brazil *Geophys. Res. Lett.* **46** 8407–14
[57] Guo Y *et al* 2018 Quantifying excess deaths related to heatwaves under climate change scenarios: a multicountry time series modelling study *PLoS Med.* **15** e1002629
[58] Peres L, Lucena A J D, Rotunno Filho O C and França J R D A 2018 The urban heat island in Rio de Janeiro, Brazil, in the last 30 years using remote sensing data *Int. J. Appl. Earth Obs.* **64** 104–16